Research Article

Hierarchical Response Network Boosts Solvent-Free Ionic Conductive Elastomers with Extreme Stretchability, Healability, and Recyclability for Ionic Sensors

Bing Zhang, Qichun Feng, Hui Song, Xu Zhang,* Chao Zhang,* and Tianxi Liu

Cite This: *ACS Appl. Mater. Interfaces* 2022, 14, 8404−8416

Read Online

ACCESS | Metrics & More | Article Recommendations | SI Supporting Information

ABSTRACT: The construction of solvent-free ionic conductive elastomers with high mechanical stretchability and large dynamic reversibility of chain segments is highly desired yet challenging. Here, a hierarchical response network strategy is presented for preparing highly stretchable yet mechanical robust ionic conductive elastomer composites (ICECs), among which poly(ethylene oxide) (PEO) microcrystalline serves as a physical cross-linking site providing high mechanical strength and elasticity, while dense hydrogen bonds endow superior mechanical toughness and dynamic reversibility. Due to the formation of the hierarchical response network, the resultant ICECs exhibit intrinsically high stretchability (>1500%), large tensile strength (~2.1 MPa), and high fracture toughness (~28 MJ m^{-3}). Intriguingly, due to the high reversibility of hydrogen-bonded networks, the ICECs after being crushed are capable of healing and recycling by simple hot-pressing for multiple cycles. Moreover, the ICECs are dissolvable under an alkaline condition and easily regenerated in an acid solution for manifold cycles. Importantly, the healed, recycled, and regenerated ICECs are capable of maintaining their initial mechanical elasticity and ionic conducting performance. Due to the integration of high stretchability, fatigue resistance, and ionic conductivity, the ICECs can readily work as a stretchable ionic conductor for skin-inspired ionic sensors for real-time and accurately sensing complex human motions. This study thus provides a promising strategy for the development of healable and renewable ionic sensing materials with high stretchability and mechanical robustness, demonstrating great potential in soft ionotronics.

KEYWORDS: *ionic conductive elastomer, hierarchical response network, extreme stretchability, recyclability, wearable ionic sensor*
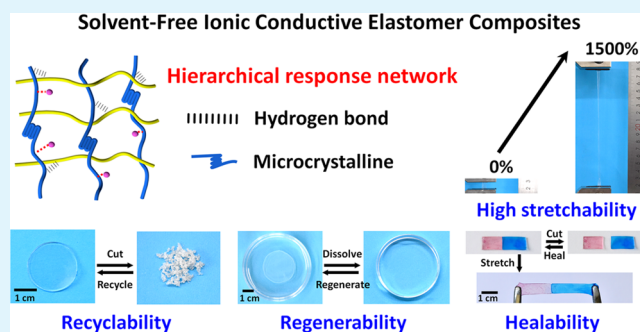
1. INTRODUCTION

Skin-inspired ionic sensors are promising wearable intelligent devices that mimic human somatosensory systems to sense external stimuli. Ionic sensors are expected to achieve functional characteristics of flexibility, transparency, and biocompatibility, which are difficult to achieve from conventional skin-inspired sensors based on electronic conductors.[1−4] Such characteristics allow the functionalization of ionic sensors for very broad application prospects in artificial intelligence, medical diagnosis, and soft robotics fields. As the most common stretchable ionic conductors, ionic conductive hydrogels and ionogels rely on the use of the salt solution and ionic liquids as ion carriers to achieve conductivity.[5,6] However, ionic conductive hydrogels suffer from functional deteriorations and poor environmental tolerances in a wide temperature range, resulting from the easy freezing or evaporation of involved water. Although ionogels have a certain degree of environmental tolerance, they still face severer bottlenecks of easy leakage and water adsorption, ascribed to the use of ionic liquids, which greatly hinder the practical applications of the currently developed stretchable

ionic conductors.[7,8] In consideration of practical applications, ionic sensors would inevitably be damaged by extrusion, scraping, and cutting, thus resulting in fatigue, fracture, and the loss of functions. These drawbacks greatly affect the stability and service life of ionic sensors, thereby leading to the waste of resources and pollution of electronic wastes.[9] The development of environmentally tolerant, healable, and renewable stretchable ionic conductors still faces a great challenge.

Ionic conductive elastomers have drawn fast-growing attention because they avoid using water or other liquid solvents. Ionic conductive elastomers are generally divided into two categories in terms of their compositions. One is composed of elastic polymers and movable ion pairs under
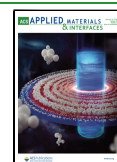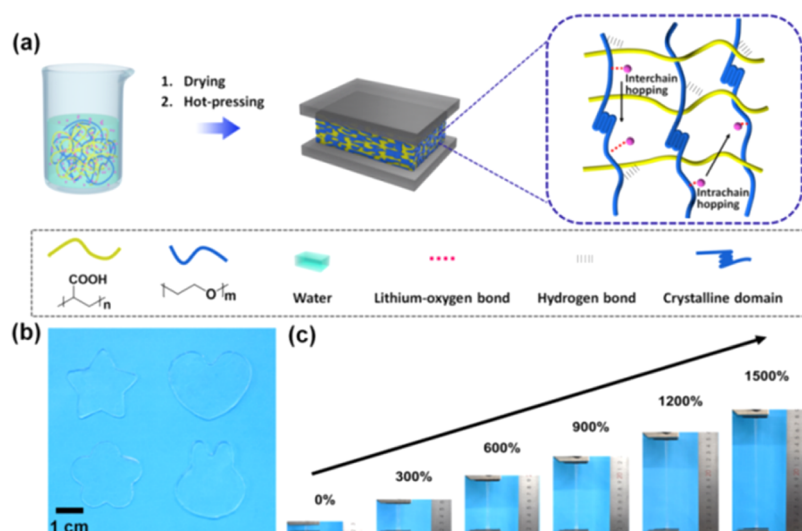
Figure 1. (a) Schematic of the fabrication process of the ICECs. (b) Photograph showing ICEC-2 being fabricated into various shapes. (c) Photograph showing ICEC-2 being stretched at a strain of 0, 300, 600, 900, 1200, and 1500%.

electric fields. Ion migrations and conductivities are achieved by the coordination and dissociation of heteroatomic functional groups (e.g., fluorine, oxygen, nitrogen) on polymer chains with the ion pairs. The other one is that the polymer matrices themselves can release free moving ions under external stimulation by the use of polymer hosts with opposite charges including poly(ionic liquid)s and polyelectrolytes. Ionic conductive elastomers have no troubles in liquid leakage and flammability because of the avoidance of flammable organic liquids, which greatly improves the safety in ionic sensing applications. Compared with inorganic ionic conductors, ionic conductive elastomers usually have flexibility, compatibility, and processability, which meet the needs of ionic sensors with both high flexibility and conductivity.[10−12] However, there is a contradiction among the ionic conductive elastomers between high stretchability and large ionic conductivity. That is, the increase in the structural stability and mechanical elasticity of ionic conductive elastomers would inevitably reduce the ion mobility within polymer matrices, thereby reducing ion conductivity. Therefore, most of the currently developed ionic conductive elastomers could not simultaneously possess excellent mechanical strength and high ionic conductivity. Moreover, the issues of mechanical damages from complex external forces (e.g., stretching, reversing, folding) make ionic conductive polymers difficult to be environmentally stable. The corresponding serious problems of source consumption and environmental wastes limit the wide-range applications of the resultant ionic conductive elastomers in ionic skin sensing.[13−15] Therefore, it is of great significance to develop highly stretchable ionic conductors with healing, renewable, and regenerative properties.

Herein, ionic conductive elastomer composites (ICECs) with hierarchical response networks have been prepared from poly(ethylene oxide) (PEO) and poly(acrylic acid) (PAA). The hierarchical response networks are composed of the simultaneous formation of physical cross-linking sites of the PEO microcrystalline and the hydrogen bonds between the PEO and PAA. The physical cross-linking sites formed by PEO microcrystalline enhance the mechanical strength and tensile resilience, while the dense hydrogen bonds between PEO and

PAA chains provide efficient energy dissipation as a "sacrificial bond" when the ICECs are subjected to external forces, endowing the ICECs with exceptional mechanical toughness and dynamic reversibility. Evenly distributed inorganic lithium salts (LiCl) not only endow the ICECs with fantastic ionic conductivity but also regulate the crystallinity of PEO as well as the resultant mechanical properties. Due to the formation of the hierarchical response network, the ICECs show high extensibility (>1500%), high tensile strength (~2.1 MPa), and great fracture toughness (~28 MJ m^{-3}). The high reversibility of dense hydrogen bonds endows the ICECs with outstanding healing, recycling, and regenerative performances. The excellent healing ability of ICECs is aided with trace water between damaged areas, and the healing efficiency is above 98% after healing for 24 h compared with the original sample. The as-prepared ICECs are capable of being recycled by simple crushing and hot-pressing, and the regenerated ICECs almost completely regain their original mechanical property and ionic conductivity. Meanwhile, the ICECs can be dissolved in an alkaline solution and further renewed by adding an acid solution. As proof-of-concept, the ICECs can work as a stretchable ionic conductor for ionic sensors, showing a high-yet-linear sensitivity in a wide strain range and high cycling stability after 1000 cycles, realizing real-time and rapid monitoring in large movements (e.g., finger/wrist bending) to small movements (e.g., airflow changing). The concept of designing hierarchical response networks in stretchable ionic conductors, therefore, paves the way for the development of highly stretchable, healable, recyclable, and regenerable ionic sensing materials in soft ionotronics.

2. EXPERIMENTAL SECTION

2.1. Materials. PAA (M_v = 450 000 g mol^{-1}), PEO (M_v = 600 000 g mol^{-1}), and LiCl (ACS reagent, ≥99%) were purchased from Aladdin. Sodium deuteroxide (NaOD, 99.5%) was purchased from Adamas. All of the chemicals were used without further purification. Deionized water was used in the experiments.

2.2. Preparation of ICECs. The aqueous solution of PEO (0.887 mmol) and PAA (0.887 mmol) was obtained by the dissolution in 53.2 and 40 mL of water, respectively. The PAA solution was gradually added into the PEO solution and stirred for 1 h. White flocculent precipitation was washed, collected, and then transferred to
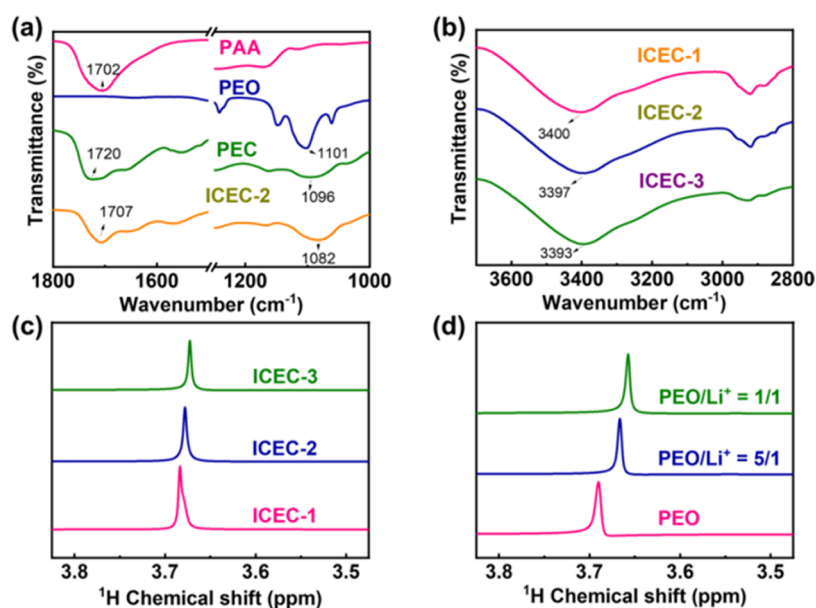
Figure 2. (a) FTIR spectra of PAA, PEO, PEC, and ICEC-2. (b) FTIR and (c) ^{1}H NMR spectra of ICECs. (d) ^{1}H NMR spectra of PEO with various Li$^+$ concentrations.

a LiCl solution under sonication. The mixture was dried in a vacuum at 60 °C for 24 h and hot-pressed under a 2 MPa pressure at 60 °C for 1 h. ICEC-1, ICEC-2, and ICEC-3 represent the ICECs with a PEO/LiCl mass ratio of 20:1, 10:1, and 5:1, respectively. For comparison, polymer elastomer composites (PECs) with various PAA/PEO molar ratios without the addition of lithium ions were prepared following the similar method for the preparation of ICECs as described above. PEC-1, PEC-2, PEC-3, PEC-4, and PEC-5 represent the feeding PAA/PEO molar ratio of 2:1, 1.5:1, 1:1, 1:1.5, and 1:2, respectively. The PAA/PEO samples were prepared from the various concentrations of PAA and PEO following the described method mentioned above for the preparation of PECs. The corresponding concentrations of the PAA/PEO were 20/20 mg mL^{-1}, 10/5 mg mL^{-1}, and 5/5 mg mL^{-1}, which are named CPEC-1, CPEC-2, and CPEC-3, respectively. For the regeneration of ICECs, after the ICECs were dissolved completely in 0.01 M NaOH, the same volume of 0.01 M HCl was also added. The obtained flocculent precipitation was washed repeatedly with water and subsequently transferred to the LiCl solution under sonication. Finally, the mixture was dried in a vacuum oven at 60 °C for 48 h and then hot-pressed for 1 h under a pressure of 2 MPa at 60 °C.

3. RESULTS AND DISCUSSION

3.1. Preparation and Structural Characterization.
ICECs were fabricated through a hierarchical response network strategy. The hierarchical response network consists of physical cross-linking networks of polymer crystallization and dense hydrogen bonds (Figure 1a). Detailed preparation procedures are given in Section 2. To obtain suitable samples, a series of comparative experiments were carried out by tailoring various monomer molar ratios, various concentrations of monomers, and various contents of inorganic salts (Figures S1 and S2). The relative mass ratio of PAA, PEO, and Li$^+$ was calculated by ^{1}H NMR, an element analyzer, and an atomic emission spectrometer (Tables S1–S3). The detailed calculation methods are shown in the Supporting Information.

The resultant ICECs were easily molded into a variety of shapes, such as a five-pointed star, heart, five-leaf clover, and rabbit head, as shown in Figure 1b. Digital photographs in Figure 1c show that ICEC-2 can be stretched to 1500% strain, demonstrating its high mechanical stretchability. The high

stretchability of ICECs could be preliminarily explained as follows. The dense hydrogen bonds were formed between the PAA and PEO chains, while the crystalline regions of PEO could also act as physical cross-linking sites. The evenly distributed inorganic lithium salts (LiCl) in the hierarchical response networks of ICECs not only endow high ionic conductivity as ion carriers but also regulate the crystallinity of PEO through the coordination with Li$^+$ ions. The hydrogen-bonded network provides an efficient energy dissipation as a "sacrificial bond" when the ICECs are subjected to external deformation, giving the ICECs exceptional mechanical toughness and recoverability. The stable physical cross-linking sites of PEO crystallization improve the mechanical strength and tensile resilience of the ICECs. For comparison, PECs were prepared from PAA and PEO using the same methods as the ICECs but without adding Li$^+$.

The hydrogen bonds between PAA and PEO, as well as the ion-coordination interactions between the Li$^+$ and PEO segments, were characterized by FTIR and ^{1}H NMR measurements. The bands at 1101 cm^{-1} in the FTIR spectra of ICECs are assigned to the vibration of ether in PEO and shift to a low wavenumber in the PECs (Figures 2a and S3). Meanwhile, a typical strong C═O vibration peak at 1702 cm^{-1} in neat PAA shifts to 1720 cm^{-1} in the PECs. The displacements of the peaks ascribing to the C═O represent the formation of hydrogen bonds among the PECs.[16,17] The absorption peaks at 3200–3600 cm^{-1} shift in the ICECs (Figure 2b). The peaks at 1147, 1060, and 1101 cm^{-1} are triple characteristic peaks of C–O–C bonds in PEO. These peaks become weakened with the increased content of Li$^+$, and the peak at 1096 cm^{-1} of neat PEC shifts to 1082 cm^{-1} among the ICEC-2. Meanwhile, the C═O vibration band of the PEC at 1720 cm^{-1} shifts to 1707 cm^{-1} of ICEC-2. These results reveal the formation of coordination interactions between the Li$^+$ ions and C–O–C in ICECs.[18–21] The Li$^+$ concentration-dependent behavior is also observed from the ^{1}H NMR spectra, wherein an upfield shifting was detected for the methylene proton signals upon increasing the Li$^+$ concentrations (Figure 2c). For comparison, neat PEO with various
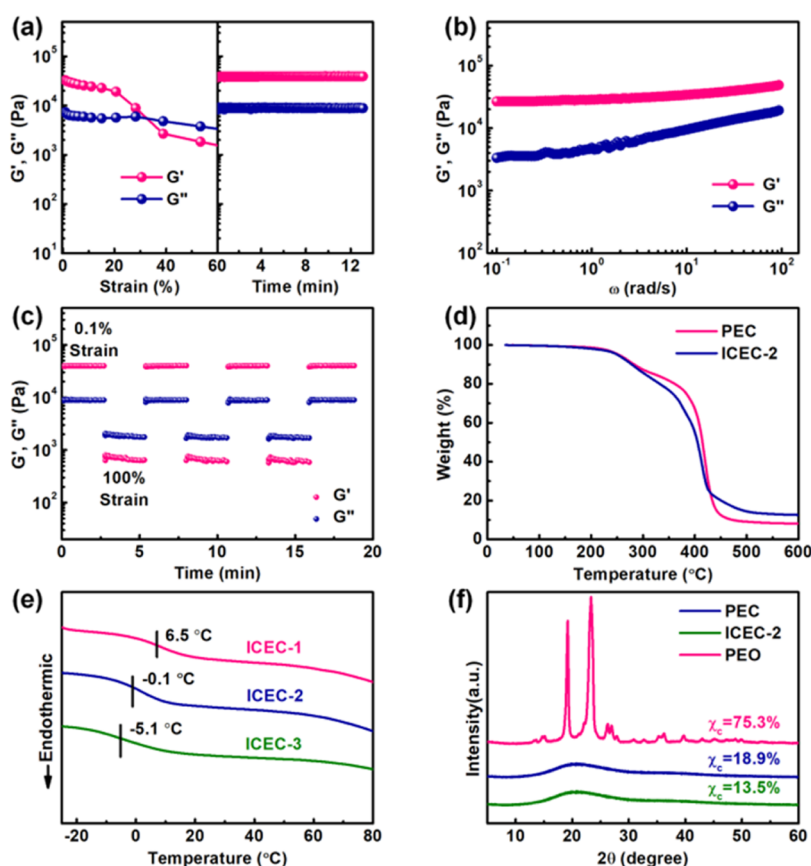
Figure 3. (a) Alternating strain−time sweep measurements of ICEC-2. (b) Frequency dependence of G' and G'' for ICEC-2 at a fixed strain of 0.5%. (c) Strain amplitude sweep test of ICEC-2 with a constant speed of 5 rad s^{-1} by varying the strain from 0.1 to 100%. (d) TGA curves of PEC and ICEC-2. (e) DSC curves of ICECs. (f) XRD patterns of PEO, PEC, and ICEC-2.

concentrations of Li$^+$ was investigated (Figure 2d), where the methylene proton signals also indicate relatively low ^{1}H chemical shifts, but the offset values are different, owing to the interactions between the Li$^+$ and oxygen atoms in the ICECs.

The rheological and viscoelastic behaviors of ICEC-2 were studied by oscillatory rheological measurements. The corresponding alternating strain−time sweep analyses are shown in Figure 3a. First, the shear strain sweep tests were measured at a fixed frequency of 5 rad s^{-1} by varying the strain from 0.1 to 100%. The storage moduli (G') and loss moduli (G'') remain constant in the low strain regions with the value of G' bigger than that of G''. The G' decreases gradually as the strain increases and then becomes lower than that of G'' when the strain exceeds 30% (left part of Figure 3a), indicating that the hydrogen bonds begin to be damaged under relatively high strain (>30%). However, when the shear strain returns to 0.1%, the G' and G'' values almost recover to the original values immediately (right part of Figure 3a), suggesting that the elastomer network is recovered rapidly. In addition to the strain, the frequency dependence of G' and G'' varying from 0.1 to 100 rad s^{-1} at a 0.5% strain was also tested, as shown in Figure 3b. During the whole frequency sweep range, the value of the G' exhibits values higher than that of G'', indicating that there exists an elastic solid-like dominant network in the examined elastomers (ICEC-2). To assess the recoverability of ICEC-2, the dynamic rheology experiment was further designed (Figure 3c). With a constant frequency of 5 rad s^{-1}, the stable behaviors of the solid state ($G' > G''$) at a relatively small shear strain of 0.1% transfer into a dynamic

liquid-like state ($G' < G''$) temporarily at a large strain of 100%. Under a 0.1% low strain, the G' and G'' values recover instantly with a quick and almost full return to their original modulus in such a short recovery time, confirming the superior fast self-recovery properties.

To evaluate the high-temperature tolerance of ICECs, the thermal gravimetric analysis (TGA) in a nitrogen atmosphere was carried out (Figure 3d). ICEC-2 exhibits a negligible weight change (only 1.1% weight loss) at 100 °C, indicating that the ICECs have high stability in conventional conditions. Furthermore, to evaluate the antifreezing performance of ICECs, glass transition temperatures (T_g) were measured by differential scanning calorimetry (DSC). Note that the ionic conductive elastomers could retain conductivity and stretchability above the T_g.[22−26] The T_g of ICEC-2 is about −0.1 °C (Figure 3e), indicating that ICEC-2 maintains stretchability and elasticity above 0 °C.[27] The crystalline structures were further investigated by X-ray diffraction (XRD). As shown in Figure 3f, XRD patterns exhibit high crystallinity of PEO,[26,28] and the enlarged view of Figure 3f of ICEC-2 is shown in Figure S4. With the addition of PAA and Li$^+$, the crystallinity degree decreases. The corresponding crystallinity degrees of PEO, PEC, and ICEC-2 were quantitatively calculated to be 75.3, 18.9, and 13.5%, respectively.

3.2. Mechanical Properties and Ionic Conductivity.
Mechanical properties of the ICECs were quantitatively measured by tensile tests at room temperature under a 100 mm min^{-1} stretching speed. Figure 4a shows a series of typical stress−strain curves of PECs and ICECs (including ICEC-1,
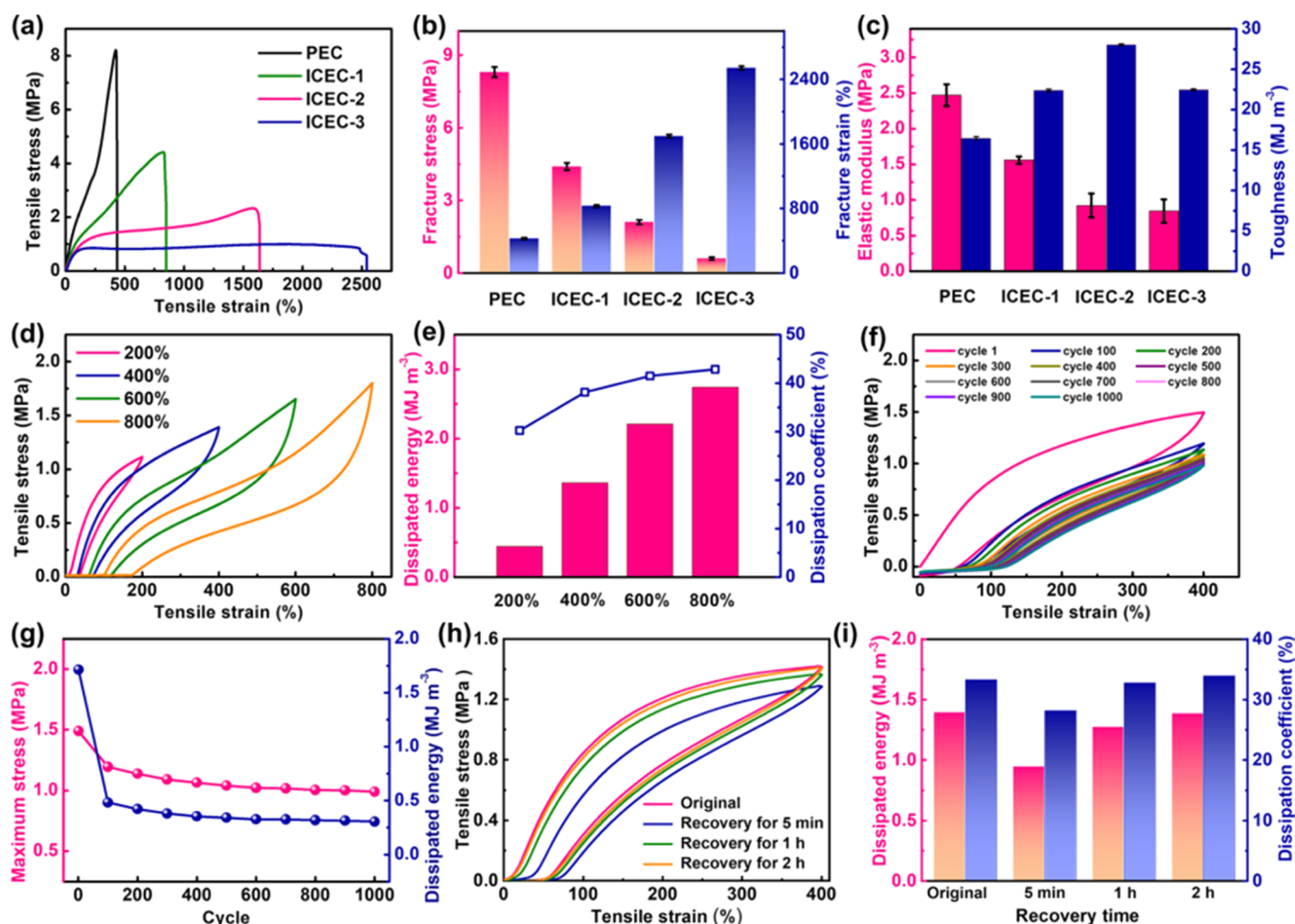
Figure 4. Mechanical properties of PEC and ICECs: (a) tensile stress−strain curves, (b) fracture stress and strain, and (c) elastic modulus and toughness. (d) Stress−strain curves of ICEC-2 at 200, 400, 600, and 800% strains. (e) Dissipated energy and energy dissipation coefficients of ICEC-2. (f) Successive tensile loading−unloading curves of ICEC-2. (g) Maximum stress and dissipated energy of ICEC-2 under successive tensile loading−unloading circles. (h) Successive recovery test of ICEC-2 at a 400% strain with various resting times. (i) Dissipated energy and energy dissipation coefficients during the recovery test with various resting times.

ICEC-2, and ICEC-3). As the content of Li⁺ increases, the fracture stress decreases from 8.3 to 0.6 MPa, and the fracture strain increases from 425 to 2542%, respectively, representing a high modulus and extreme stretchability (Figure 4b). With the increased content of Li⁺, the ICECs become ductile and the corresponding elastic modulus decreases, while the toughness increases first to an optimal value (for ICEC-2) and then decreases (Figure 4c). Considering the high tensile strength and toughness, ICEC-2 was chosen as a representative material for the following investigations. It can be concluded from the tensile tests that the as-prepared ICECs exhibit high mechanical strength and stretchability, owing to the reversibility of the dense hydrogen-bonded network and the crystalline physical cross-linking network,[29] which can be further addressed by in situ attenuated total reflection (ATR)-FTIR spectroscopy (Figure S5). Both sides of the tensile samples for the FTIR measurements were fixed to the tensile fixture of the tensile testing machine, and the middle position of the stretched sample was monitored with the FTIR instrument probe. As the strain increases from 50 to 400%, the intensity of the infrared absorption peaks of −OH increases, indicating that the hydrogen bonds are partially destroyed during the stretching.

To assess the toughness, the energy dissipation was further evaluated through the loading−unloading tests, where the samples were first stretched and then recovered at the same speed. Figure 4d displays the loading−unloading curves of ICEC-2 at a strain of 200, 400, 600, and 800%, respectively. It can be observed that the loading−unloading profiles exhibit the apparent hysteresis loops, indicating that the ICECs could effectively dissipate the tensile energy due to the reversible breaking of the hydrogen-bonded network. The corresponding quantified results are also shown in Figure 4e, where the energy dissipation (dissipation coefficient) at a 200, 400, 600, and 800% strain are 444.4, 1363.9, 2209.7, and 2741.6 kJ m⁻³ (30.3, 38.1, 41.5, and 42.9%), respectively. The energy dissipation and dissipation coefficient of the loading−unloading cycles increase simultaneously as the tensile strain increases, indicating that more hydrogen bonds in the network are destroyed at the relatively higher tensile strain.

The antifatigue property of ICEC-2 was further investigated by performing successive 1000 cyclic loading−unloading tensile tests at a 400% strain without interval (Figure 4f). A large hysteresis loop appears in the first cycle due to the reversible interactions. Nevertheless, subsequent cycles exhibit relatively small hysteresis loops as a consequence of the reversible hydrogen bonds. As shown in Figure 4g, the
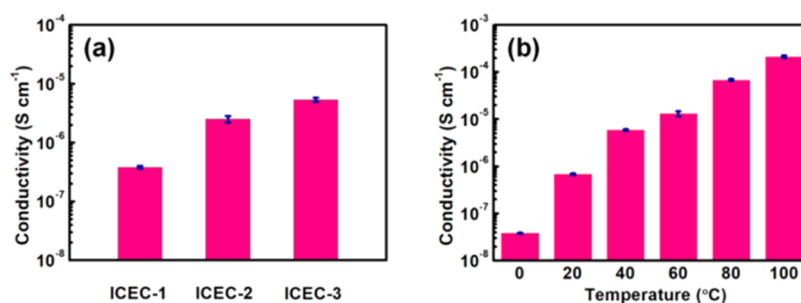
Figure 5. (a) Ionic conductivity of ICEC-1, ICEC-2, and ICEC-3. (b) Effect of temperature on ionic conductivity of ICEC-2.
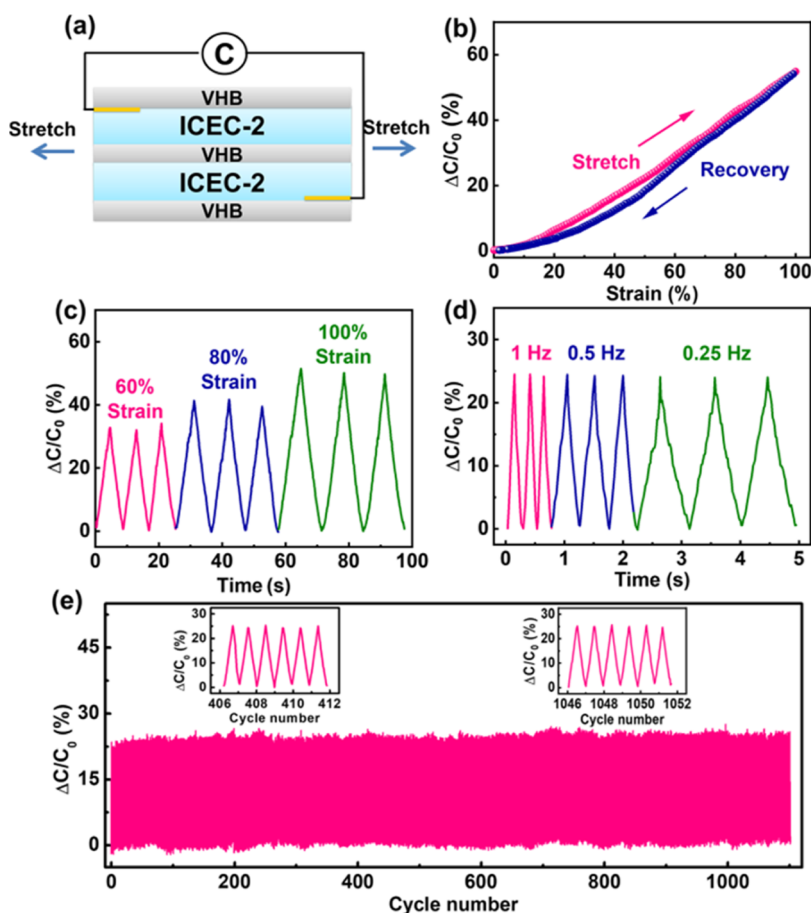

Figure 6. Sensing performances of ICEC-2 in a capacitive ionic sensor. (a) Schematic of the assembly of the sensor. (b) Reversible capacitance−strain curves. Relative capacitance changes of the sensor under various (c) strains and (d) frequencies. (e) Cycling stability of relative capacitive changes for the sensor.

dissipation energy decreases from 1713.3 kJ m^{-3} for the 1st cycle to 482.5 kJ m^{-3} for the 2nd cycle and then slightly decreases, i.e., 380.6, 354.6, and 305.4 kJ m^{-3}, for the 4th, 5th, and 10th cycle, respectively. Also, the maximum stress slightly decreases from the second cycle. The self-recovery property could be observed between two loading−unloading cycles under 400% strain with various resting times (Figure 4h). The tensile stress−strain curves of ICEC-2 return to the original state after resting for 2 h at a 400% strain. The corresponding dissipated energy and the dissipation coefficient recover to 1.4 MJ m^{-3} and 33%, approaching the original values of 1.4 MJ m^{-3} and 33% (Figure 4i), respectively. ICEC-2 is capable of recovering to its original value at a small stain immediately (Figure S6). After resting for 3 min, the dissipated energy and the dissipation coefficient of ICEC-2, respectively, recover to

16.7 kJ m^{-3} and 22.2%, approaching each original value (21.3 kJ m^{-3} and 24.4%). The outstanding self-recovery and fatigue resistance of ICEC-2 could be reasonably attributed to the reversible hydrogen-bonded network.[30−35]

In addition to the good mechanical properties, the as-prepared ICECs also have good ionic conductivity compared to most of the currently developed ionic conductive elastomers (Table S4). The effect of the mass ratio of the elastomers to LiCl on the ionic conductivity is shown in Figure 5a. With the decrease in the mass ratio of PEO to LiCl from 20/1 (ICEC-1) to 10/1 (ICEC-2) and then to 5/1 (ICEC-3) or the increase in the salt content, the ionic conductivity increases from 3.8×10^{-7} to 2.5×10^{-6} and then to 5.4×10^{-6} S cm^{-1}, respectively. The increase in ionic conductivity is attributed to the increased density of ion carriers when loading more salts.[36] Moreover,
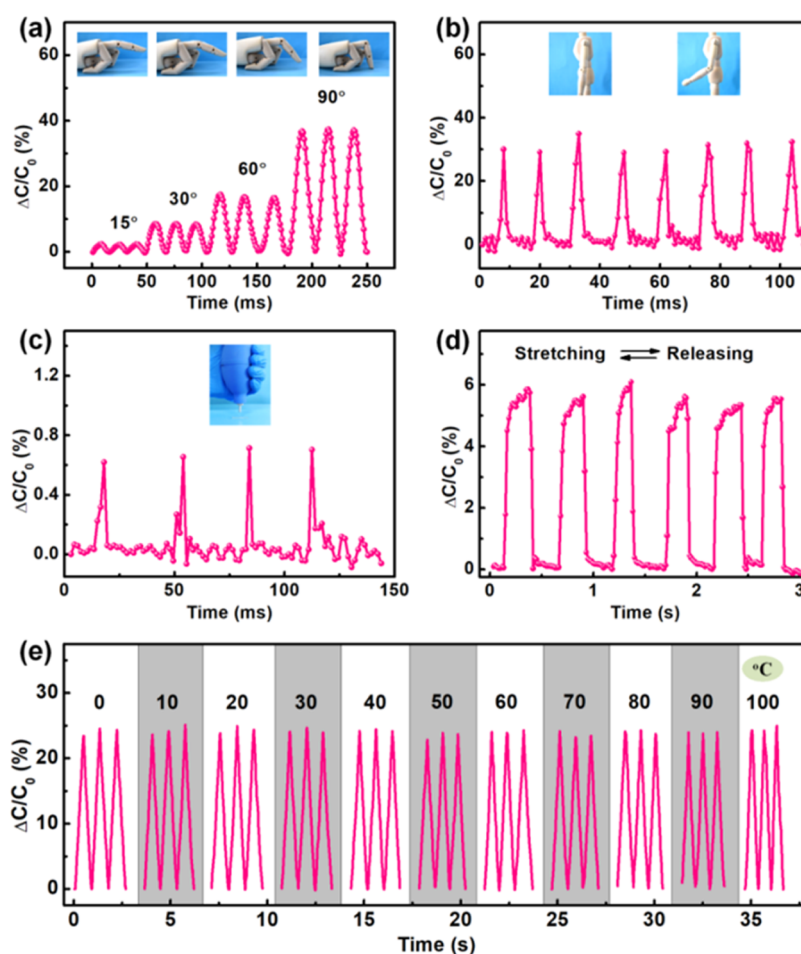
Figure 7. Real-time capacitance signals of the ICEC-2 sensor in detecting (a) finger bending, (b) wrist bending, and (c) changes in the airflow. Insets of (a−c) are photographs captured during the corresponding measurements. (d) Relative capacitive changes of the ICEC-2 sensor under stretching cycles. (e) Relative capacitive variations of the ICEC-2 sensor at various temperatures.

the ionic conductivity of the ICECs also reveals the temperature dependence, as shown in Figure 5b. Taking ICEC-2 as an example, the ionic conductivity of ICEC-2 gradually increases from 3.8×10^{-8} to 2.1×10^{-4} S cm^{-1} as the temperature increases from 0 to 100 °C. It can be attributed to the fact that the higher temperature leads to more efficient mobility of polymer segments and free removable ions, resulting in higher ionic conductivity. Note that the ionic conductivity is proportional to the effective number of movable ions.[37−39]

3.3. Demonstration as a Stretchable Conductor in Strain Sensors. Benefiting from the high mechanical performance and large ionic conductivity compared to the currently developed ionic conductive elastomers in the literature (Tables S4 and S5), ICEC-2 is an ideal candidate material for preparing soft ionotronic devices. Based on this inspiration, ion-based elastomers were assembled into a sandwich-structured capacitive sensor (Figure 6a), consisting of an acrylic elastomer (3M VHB 4905) as a dielectric layer between two ICEC-2 ionic conductors. In addition to the dielectric layer, VHB films with high elasticity and self-adhering performance adhered to the other two sides of ionic conductors before measurements. Two electrodes were connected to a capacitive meter by two steel wires. The capacitance signals were recorded when the external stimuli (i.e., pressure, stretching, and bending) are applied to the ionic

sensor. Figure 6b displays the reversible linear relationship between the capacitance and strain. The strain sensitivity of the capacitive sensors could be obtained by the slope of the curves, where C_0 and C ($\Delta C = C - C_0$) are the initial capacitance and the capacitance under stretching, respectively. Figure 6c shows the relative capacitive change ($\Delta C/C_0$) curves of ICEC-2 sensors under the stepped cyclic stretched strain. It can be found from Figure 6c that the relative capacitive changes at different strains (60, 80, and 100%) almost recover to the original value completely, demonstrating that the as-prepared capacitive sensors have excellent strain-sensing reversibility.[40] When the periodic stretching with a 50% strain at various frequencies of 1, 0.5, and 0.25 Hz is performed (Figure 6d), the sensing output signals follow the negligible changes both in the shape and peak, which further clarifies the accuracy of the ICEC-2 sensors upon being applied with external stimuli at different frequencies. Figure 6e shows the fatigue evaluation of the sensors, where a periodic strain of 50% is applied and released for over 1000 cycles. Two insets in Figure 6e further confirm that the strain sensors are resistant for long-term uses with excellent stability and durability without signal depression.[39,41−43]

As next-generation sensing devices, strain sensors have been becoming popular due to their potential applications in advanced artificial intelligence, medical diagnosis, and software robots. The ICEC-2 strain sensors have high performances in
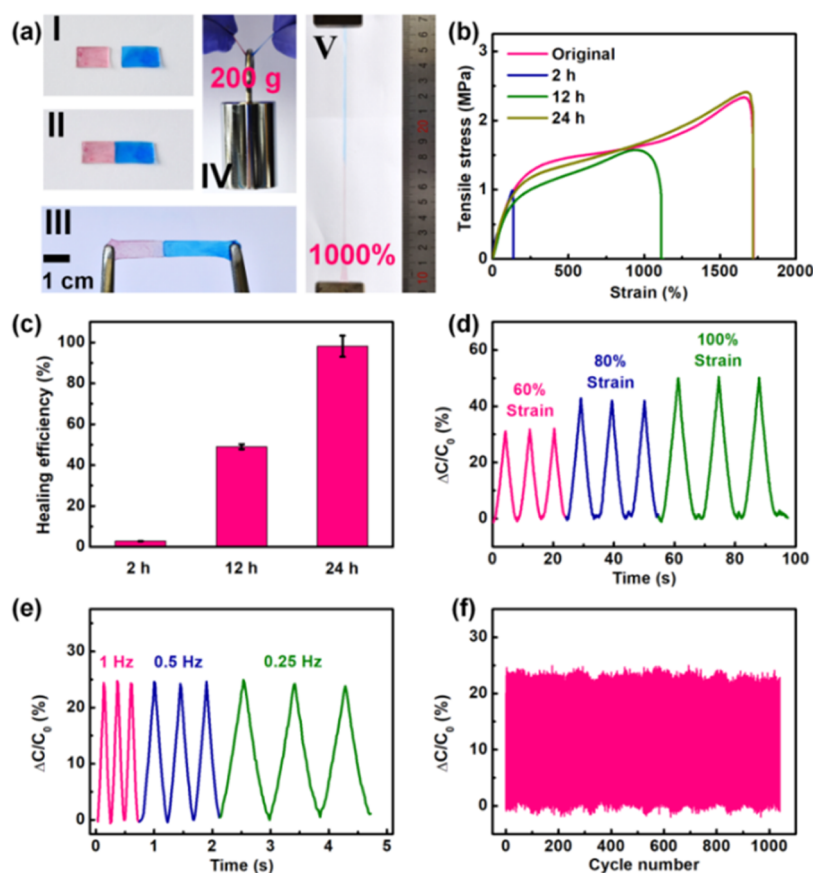
Figure 8. Healing performances of ICEC-2. (a) Digital photographs of the undyed and dyed samples being cut into two pieces (I), well-healed (II), stretched after healing (III), holding a weight of 200 g (IV), and stretched to 1000% strain without fracture (V). (b) Stress–strain curves of the original and healed ICEC-2 for various healing times. (c) Healing efficiency after various healing times. Relative capacitance changes of healed ICEC-2 under various (d) strains and (e) frequencies. (f) Cycling stability of relative capacitive changes for healed ICEC-2.

detecting large strains of human finger joints and elbows (Figure 7a,b). The assembled capacitive sensors including the VHB film could be adhered to finger joints and elbows of a volunteer by adhesive tapes. It can recognize the bending of finger joints at 15, 30, 60, and 90°, respectively. The signals accordingly change in the relative capacitive of the sensors as the bending angle increases from 15 to 90°, and the output signals are highly repeatable and stable, as shown in Figure 7a. Similarly, when the strain sensors are attached to the elbows, the signals could sense the bending direction of the elbows, as shown in Figure 7b. The sensor could also distinguish subtle changes in the airflow (Figure 7c). The subtle changes in the airflow were detected by placing the washing ear ball above the sensor and blowing the air intermittently. The slight stretching and releasing signals were also detected by simply holding both ends of the sensor and stretching the sensor with a small force (Figure 7d). The high applicability in a wide temperature range has been further investigated using ICEC-2 at various temperatures (Figure 7e). The stable and repeatable relative capacitive changes under 50% strain at the temperature ranging from 0 to 100 °C in Figure 7e confirm that the ICEC-2 sensors possess excellent resilience and capacitive stability over a wide temperature range.[37,44,45]

3.4. Healing and Recycling Performance. Not just the mechanical and strain-sensing properties, the current designed ICECs also show excellent healing and recycling properties, owing to the reversible dynamic dense hydrogen bonds and the ionic coordination interactions, as shown in Figure 8. Two

ICEC-2 cuboids were fabricated, with one dyed orange and the other one blue (I in Figure 8a). These two pieces of differently colored ICEC-2 were then brought into contact with different times to achieve healing from damage at room temperature, in which a small amount of deionized water was added into the fractured interfaces (II in Figure 8a). After healing for 24 h and vacuum drying at 60 °C for 24 h, the healed ICEC-2 could be stretched without fracture (III in Figure 8a). In addition, the healed ICEC-2 is capable of holding a weight of 200 g (IV in Figure 8a) and being stretched to 1000% strain without secondary damage (V in Figure 8a) as the original ICEC-2. The healing efficiencies were quantified through the tensile tests (Figure 8b), and the samples were dried under vacuum before testing. The healing efficiency is defined as the ratio of the fracture toughness of healed samples to the original fracture toughness. The 24 h-healed samples could almost recover to the initial mechanical properties and the healing efficiency reaches about 98% (Figure 8c), where the intrinsic reliability of the healing performance is because there are a large number of hydrogen bonds and ionic coordination interactions across the interfaces.[28,46,47] Most notably, taking advantage of the healing ability of the ICECs, it can be stated that the ICEC-based sensors are capable of fully recovering to the original sensing ability, as shown in Figure 8d,e, where the relative capacitive curves under different strains and frequencies almost follow the original curve. Additionally, the sensing stability of the 24 h-healed ICEC-2 sensors over 1000 cycles (Figure 8f) is similar to the original sensors. These
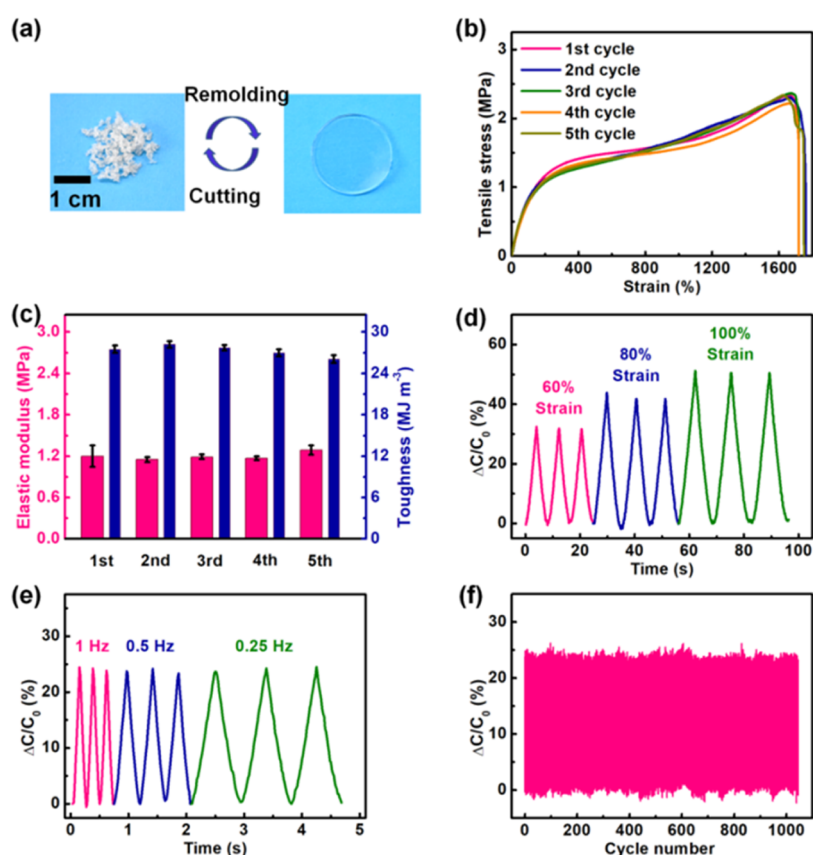
Figure 9. (a) Photographs showing the cutting and remodeling cycles of ICEC-2 by hot-pressing. (b) Stress−strain curves of recycled ICEC-2 for the various cutting−remodeling cycles. (c) Corresponding modulus and toughness of recycled ICEC-2 from (d). Relative capacitance changes of recycled ICEC-2 under various (d) strains and (e) frequencies. (f) Cycling stability of relative capacitive changes for the fifth recycled ICEC-2.

results indicate that the sensing ability of the ICEC-2 sensors is completely regained after the cutting−healing process.

ICEC-2 could also be recycled for repeated uses. As proof-of-concept, the recyclable performance is proven through the cutting−remolding process, where the samples are cut into millimeter-sized pieces and then remolded into coherent samples (Figure 9a). After being remolded under a pressure, a piece of circular-shaped ICEC-2 is reobtained, and then stress−strain curves of the recycled ICEC-2 are evaluated and shown in Figure 9b. It can be seen from Figure 9b that the recycled ICEC-2 can retain its original mechanical strength during five cycles of the cutting−remolding process. The elastic modulus and toughness of the first, second, third, fourth, and fifth cycles (Figure 9c) are almost overlapped compared with the original mechanical strength. Moreover, the ionic conductivity of ICEC-2 for the first, second, and fifth cycles of the cutting−remolding process was 2.5×10^{-6}, 2.2×10^{-6}, and 2.3×10^{-6} S cm^{-1}, respectively (Figure S7). The recycled ICEC-2 can recuperate most of the initial mechanical properties during five cycles of the cutting−remolding process, confirming that the as-prepared ICECs possess excellent recyclability and reprocessability.[48,49] The environmental stability of ICEC-2 in the open-air and high-humidity environments was investigated. Figure S8a shows that the residual weight of ICEC-2 remains almost unchanged after 1 day and increases a little after 7 days in open-air (~46% RH, ~19 °C) environments. Figure S8b shows that the weight of ICEC-2 increases a little and then remains unchanged under a high-humidity (~72% RH, ~16 °C) environment.

The sensing ability of the fifth recycled ICEC-2 is further examined to evaluate the reproducibility of the as-prepared ICEC-2; the real-time responses of the fifth recycled ICEC-2 flexible devices were investigated by quick loading−unloading at 60, 80, and 100% strain with three circles (Figure 9d). When the periodic loading−unloading process at 50% strain is applied under various frequencies of 1, 0.5, and 0.25 Hz (Figure 9e), the strain-sensing output signals show negligible changes, illustrating that the fifth recycled ICEC-2 still maintains accurate sensing ability under various stimuli, including strain and frequency. Figure 9f shows the stability of the sensors when a periodic 50% strain is applied and released over 1000 cycles, confirming that the strain sensors can be endured over a long time with excellent stability and durability without obvious signal depression. Most noteworthy, there is no significant difference in the strain-sensing performance between the fifth recycled ICEC-2 and the original ICEC-2 being recycled even under different strains, frequencies, and cycles.

3.5. Dissolvable and Regenerative Properties. A dissolvable and regenerative elastomer is highly desirable to alleviate plastic pollution resulting from the improper management of typically "long-lived" synthetic organic polymers or inferior recycling. In the present work, the dissolvable and regenerative properties of ICEC-2 are further investigated. ICEC-2 can be dissolved steadily in an alkaline solution. For example, ICEC-2 can be dissolved completely in 1 M NaOH (Figure 10a). As the infiltration time increases, the ICECs are dissolved gradually and disappear completely after 8 h. After
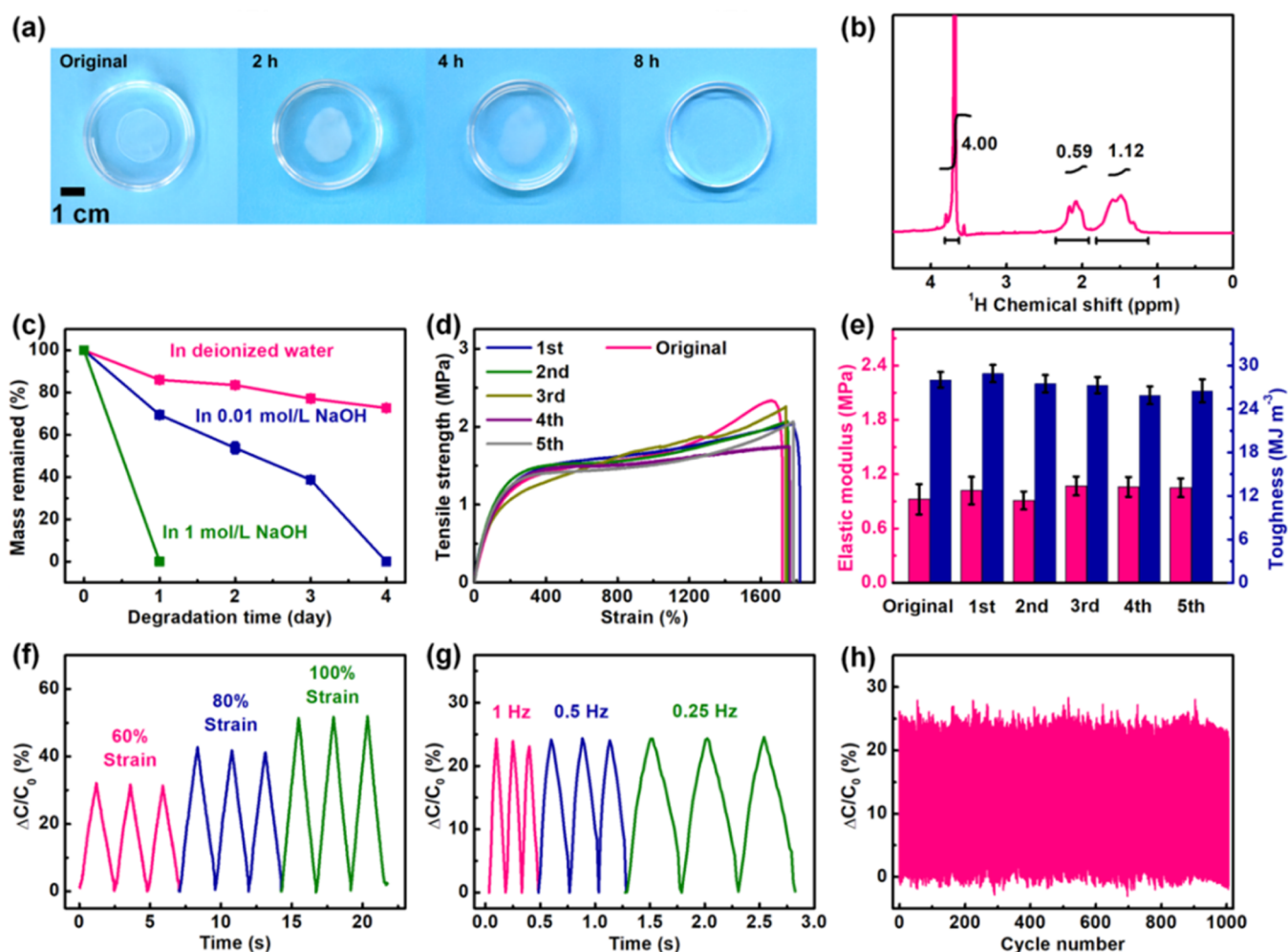
Figure 10. (a) Photographs showing the dissolution process of ICEC-2 in 1 M NaOH. (b) ^{1}H NMR spectrum of ICEC-2 after being soaked in 1 M NaOH for 10 min and then dissolved in D_2O. (c) Dissolution of ICEC-2 in water, 0.01 M NaOH, and 1 M NaOH at 25 °C. (d) Stress−strain curves of the original and ICEC-2 after various dissolving−regenerating cycles. (e) Elastic modulus and toughness of the original and ICEC-2 after various dissolving−regenerating cycles. Relative capacitance changes of five cycle-regenerated ICEC-2 under various (f) strains and (g) frequencies. (h) Cycling stability of relative capacitive changes for five cycle-regenerated ICEC-2.

immersing in 1 M NaOH for 10 min, the residual ICEC-2 is vacuum dried and redissolved in deuterium oxide (D_2O), and then quantitatively analyzed by ^{1}H NMR. The relative molar ratio of PAA to PEO decreases to 0.59:1 (Figure 10b), which indicates the rapid dissolution in a short time in an alkali solution.[50,51] For comparison, the deionized water and a 0.01 M NaOH solution are also used here at ambient temperature to observe the dissolution process (Figure 10c). There is a slow dissolution process in deionized water because the hydrogen bonds are difficult to be broken in pure water. While in 0.01 M NaOH, the dissolution could be accomplished after 4 days, which is lower than that in 1 M NaOH (1 day).

Interestingly, the flocculent precipitation was reproduced again when ICEC-2 in a NaOH solution was neutralized by a HCl solution after complete dissolution. ICEC-2 could be reobtained and can be further reused from the flocculent precipitation after washing, collecting, and then transferring to a LiCl solution, which is similar to the preparation method of the ICECs presented above in Section 2. This renewable ICEC-2 can regain the original mechanical strength after five dissolving−regenerating cycles (Figure 10d), including the elastic modulus and toughness (Figure 10e). The regenerative mechanism is attributed to the presence of reversible dynamic

dense hydrogen bonds.[52] The sensing ability of the regenerated ICEC-2 over five dissolving−regenerating circles was further elevated, showing the relative capacitive changes under different strains (Figure 10f) and frequencies at 50% strain (Figure 10g) of the fifth regenerated ICEC-2 are completely consistent with the original ICEC-2. In addition, the sensing stability of the fifth regenerated ICEC-2 over 1000 cycles at a 50% strain (Figure 10h) is also similar to that of the original ICEC-2. It can be concluded from the above mentioned results that the as-prepared ICECs own unique dissolvable and regenerative properties.

4. CONCLUSIONS

In summary, the ICECs with high mechanical strength and extreme stretchability have been prepared through a hierarchical response network strategy based on the formation of physical cross-linking networks of PEO microcrystalline and dense hydrogen bonds. Benefitting from the formation of the hierarchical response network in the ICECs, the resultant ionic elastomer composites combine high mechanical elasticity (e.g., large stretchability, high toughness, high fatigue resistance) with high ionic conductivity compared to previously developed

ionic conductive elastomers. Ascribed to the high reversibility of dense hydrogen bonds, the ICECs exhibit high-efficiency water-aided healability and recyclability by simple crushing and hot-pressing. The ICECs are capable of being regenerated in a solution-processing way, which can be rapidly dissolved in an alkaline solution and regenerated by adding an acid solution. The recycled and regenerated ICECs can retain excellent mechanical properties that are comparable to their original states. Importantly, the ICECs are capable of maintaining high ionic conductivity that is comparable to previously developed ionic conductive elastomers, allowing them to serve as a stretchable ionic conductor for ionic sensors, showing high sensitivity and durability in accurately monitoring both large-range and small-strain movements in the detection of human motions of finger bending, wrist flexion, and airflow changing. It could be envisioned that the hierarchical response network strategy provides a new path for preparing stretchable ionic conductors with high mechanical strength, high sensitivity, and outstanding durability in a wide temperature range for skin-inspired ionic sensors.

■ ASSOCIATED CONTENT

ⓈⒾ Supporting Information

The Supporting Information is available free of charge at https://pubs.acs.org/doi/10.1021/acsami.1c22602.

> Characterizations; calculation of the relative molar ratio and the mass ratio; relative mass content of Li^+, PAA, and PEO in ICECs; ^1H NMR spectra of PEC, DPEC, and IPEC; FTIR spectra of PAA and PEC; XRD patterns of ICEC-2; FTIR spectra of ICEC-2 stretched at various strains; recovery test of ICEC-2 under 40% strain with various resting times; dissipated energy and energy dissipation coefficients of ICEC-2 during the recovery test; ionic conductivity of ICEC-2 for various remodeling cycles; environmental stability of ICEC-2 in open-air and high-humidity environments; summary of relative molar ratios of PAA and PEO in PECs (Table S1); summary of relative molar ratios of PAA and PEO in ICECs (Table S2); summary of relative element contents in ICECs (Table S3); summary of ionic conductivity of ionic conductive elastomers in the literature (Table S4); and summary of mechanical properties and sensing performances of ionic conductive elastomers in the literature (Table S5) (PDF)

■ AUTHOR INFORMATION

Corresponding Authors

Xu Zhang − *State Key Laboratory for Modification of Chemical Fibers and Polymer Materials, College of Materials Science and Engineering, Innovation Center for Textile Science and Technology, Donghua University, Shanghai 201620, P. R. China*; Email: xuzhang@dhu.edu.cn

Chao Zhang − *State Key Laboratory for Modification of Chemical Fibers and Polymer Materials, College of Materials Science and Engineering, Innovation Center for Textile Science and Technology, Donghua University, Shanghai 201620, P. R. China*; orcid.org/0000-0003-1255-7183; Email: czhang@dhu.edu.cn

Authors

Bing Zhang − *State Key Laboratory for Modification of Chemical Fibers and Polymer Materials, College of Materials*

Science and Engineering, Innovation Center for Textile Science and Technology, Donghua University, Shanghai 201620, P. R. China

Qichun Feng − *State Key Laboratory for Modification of Chemical Fibers and Polymer Materials, College of Materials Science and Engineering, Innovation Center for Textile Science and Technology, Donghua University, Shanghai 201620, P. R. China*

Hui Song − *State Key Laboratory for Modification of Chemical Fibers and Polymer Materials, College of Materials Science and Engineering, Innovation Center for Textile Science and Technology, Donghua University, Shanghai 201620, P. R. China*

Tianxi Liu − *State Key Laboratory for Modification of Chemical Fibers and Polymer Materials, College of Materials Science and Engineering, Innovation Center for Textile Science and Technology, Donghua University, Shanghai 201620, P. R. China; Key Laboratory of Synthetic and Biological Colloids, Ministry of Education, School of Chemical and Material Engineering, Jiangnan University, Wuxi 214122, P. R. China*; orcid.org/0000-0002-5592-7386

Complete contact information is available at:
https://pubs.acs.org/10.1021/acsami.1c22602

Author Contributions

This manuscript was written through contributions of all authors. All authors have given approval to the final version of the manuscript.

Notes

The authors declare no competing financial interest.

■ ACKNOWLEDGMENTS

■ REFERENCES

(1) Xiao, K.; Wan, C.; Jiang, L.; Chen, X.; Antonietti, M. Bioinspired Ionic Sensory Systems: The Successor of Electronics. *Adv. Mater.* **2020**, *32*, No. 2000218.

(2) Wang, Z.; Cong, Y.; Fu, J. Stretchable and Tough Conductive Hydrogels for Flexible Pressure and Strain Sensors. *J. Mater. Chem. B* **2020**, *8*, 3437−3459.

(3) Wang, Y.; Cao, X.; Cheng, J.; Yao, B.; Zhao, Y.; Wu, S.; Ju, B.; Zhang, S.; He, X.; Niu, W. Cephalopod-Inspired Chromotropic Ionic Skin with Rapid Visual Sensing Capabilities to Multiple Stimuli. *ACS Nano* **2021**, *15*, 3509−3521.

(4) Shang, Y.; Wu, C.; Hang, C.; Lu, H.; Wang, Q. Hofmeister-Effect-Guided Ionohydrogel Design as Printable Bioelectronic Devices. *Adv. Mater.* **2020**, *32*, No. 2000189.

(5) Lei, Z.; Wu, P. A Highly Transparent and Ultra-Stretchable Conductor with Stable Conductivity During Large Deformation. *Nat. Commun.* **2019**, *10*, No. 3429.

(6) Yang, Q.; Wei, T.; Yin, R. T.; Wu, M.; Xu, Y.; Koo, J.; Choi, Y. S.; Xie, Z.; Chen, S. W.; Kandela, I.; Yao, S.; Deng, Y.; Avila, R.; Liu, T. L.; Bai, W.; Yang, Y.; Han, M.; Zhang, Q.; Haney, C. R.; Benjamin Lee, K.; Aras, K.; Wang, T.; Seo, M. H.; Luan, H.; Lee, S. M.; Brikha, A.; Ghoreishi-Haack, N.; Tran, L.; Stepien, I.; Aird, F.; Waters, E. A.; Yu, X.; Banks, A.; Trachiotis, G. D.; Torkelson, J. M.; Huang, Y.; Kozorovitskiy, Y.; Efimov, I. R.; Rogers, J. A. Photocurable Bioresorbable Adhesives as Functional Interfaces between Flexible

Bioelectronic Devices and Soft Biological Tissues. *Nat. Mater.* **2021**, *20*, 1559−1570.

(7) Qian, W.; Texter, J.; Yan, F. Frontiers in Poly(Ionic Liquid)s: Syntheses and Applications. *Chem. Soc. Rev.* **2017**, *46*, 1124−1159.

(8) Liang, W.; Chen, J.; Li, L.; Li, M.; Wei, X.; Tan, B.; Shang, Y.; Fan, G.; Wang, W.; Liu, W. Conductive Hydrogen Sulfide-Releasing Hydrogel Encapsulating Adscs for Myocardial Infarction Treatment. *ACS Appl. Mater. Interfaces* **2019**, *11*, 14619−14629.

(9) Zheng, N.; Xu, Y.; Zhao, Q.; Xie, T. Dynamic Covalent Polymer Networks: A Molecular Platform for Designing Functions Beyond Chemical Recycling and Self-Healing. *Chem. Rev.* **2021**, *121*, 1716−1745.

(10) Li, C.-H.; Wang, C.; Keplinger, C.; Zuo, J.-L.; Jin, L.; Sun, Y.; Zheng, P.; Cao, Y.; Lissel, F.; Linder, C.; You, X.-Z.; Bao, Z. A Highly Stretchable Autonomous Self-Healing Elastomer. *Nat. Chem.* **2016**, *8*, 618−624.

(11) Amoli, V.; Kim, J. S.; Kim, S. Y.; Koo, J.; Chung, Y. S.; Choi, H.; Kim, D. Ionic Tactile Sensors for Emerging Human-Interactive Technologies: A Review of Recent Progress. *Adv. Funct. Mater.* **2020**, *30*, No. 1904532.

(12) Rahman, S. S.; Arshad, M.; Qureshi, A.; Ullah, A. Fabrication of a Self-Healing, 3D Printable, and Reprocessable Biobased Elastomer. *ACS Appl. Mater. Interfaces* **2020**, *12*, 51927−51939.

(13) Deng, Z.; Wang, H.; Ma, P. X.; Guo, B. Self-Healing Conductive Hydrogels: Preparation, Properties and Applications. *Nanoscale* **2020**, *12*, 1224−1246.

(14) Ruan, K.; Shi, X.; Guo, Y.; Gu, J. Interfacial Thermal Resistance in Thermally Conductive Polymer Composites: A Review. *Compos. Commun.* **2020**, *22*, No. 100518.

(15) Nezakati, T.; Seifalian, A.; Tan, A.; Seifalian, A. M. Conductive Polymers: Opportunities and Challenges in Biomedical Applications. *Chem. Rev.* **2018**, *118*, 6766−6843.

(16) Zhang, W.; Wu, B.; Sun, S.; Wu, P. Skin-Like Mechanoresponsive Self-Healing Ionic Elastomer from Supramolecular Zwitterionic Network. *Nat. Commun.* **2021**, *12*, No. 4082.

(17) Li, R. A.; Zhang, K. L.; Chen, G. X.; Su, B.; He, M. H. Stiff, Self-Healable, Transparent Polymers with Synergetic Hydrogen Bonding Interactions. *Chem. Mater.* **2021**, *33*, 5189−5196.

(18) Qiao, H.; Qi, P.; Zhang, X.; Wang, L.; Tan, Y.; Luan, Z.; Xia, Y.; Li, Y.; Sui, K. Multiple Weak H-Bonds Lead to Highly Sensitive, Stretchable, Self-Adhesive, and Self-Healing Ionic Sensors. *ACS Appl. Mater. Interfaces* **2019**, *11*, 7755−7763.

(19) Yang, C.-T.; Lin, Y.-X.; Li, B.; Xiao, X.; Qi, Y. The Bonding Nature and Adhesion of Polyacrylic Acid Coating on Li-Metal for Li Dendrite Prevention. *ACS Appl. Mater. Interfaces* **2020**, *12*, 51007−51015.

(20) Guo, Y.; Qu, X.; Hu, Z.; Zhu, J.; Niu, W.; Liu, X. Highly Elastic and Mechanically Robust Polymer Electrolytes with High Ionic Conductivity and Adhesiveness for High-Performance Lithium Metal Batteries. *J. Mater. Chem. A* **2021**, *9*, 13597−13607.

(21) Niu, W.; Zhu, Y.; Wang, R.; Lu, Z.; Liu, X.; Sun, J. Remalleable, Healable, and Highly Sustainable Supramolecular Polymeric Materials Combining Superhigh Strength and Ultrahigh Toughness. *ACS Appl. Mater. Interfaces* **2020**, *12*, 30805−30814.

(22) Yiming, B.; Guo, X.; Ali, N.; Zhang, N.; Zhang, X.; Han, Z.; Lu, Y.; Wu, Z.; Fan, X.; Jia, Z.; Qu, S. Ambiently and Mechanically Stable Ionogels for Soft Ionotronics. *Adv. Funct. Mater.* **2021**, *31*, No. 2102773.

(23) Wang, H.; Liu, H.; Cao, Z.; Li, W.; Huang, X.; Zhu, Y.; Ling, F.; Xu, H.; Wu, Q.; Peng, Y.; Yang, B.; Zhang, R.; Kessler, O.; Huang, G.; Wu, J. Room-Temperature Autonomous Self-Healing Glassy Polymers with Hyperbranched Structure. *Proc. Natl. Acad. Sci. U.S.A.* **2020**, *117*, 11299−11305.

(24) Xu, S. J.; Sun, Z. H.; Sun, C. G.; Li, F.; Chen, K.; Zhang, Z. H.; Hou, G. J.; Cheng, H. M.; Li, F. Homogeneous and Fast Ion Conduction of PEO-Based Solid-State Electrolyte at Low Temperature. *Adv. Funct. Mater.* **2020**, *30*, No. 2007172.

(25) Gao, Y.; Jia, F.; Gao, G. Ultra-Thin, Transparent, Anti-Freezing Organohydrogel Film Responded to a Wide Range of Humidity and Temperature. *Chem. Eng. J.* **2022**, *430*, No. 132919.

(26) Hou, K. X.; Zhao, S. P.; Wang, D. P.; Zhao, P. C.; Li, C. H.; Zuo, J. L. A Puncture-Resistant and Self-Healing Conductive Gel for Multifunctional Electronic Skin. *Adv. Funct. Mater.* **2021**, *31*, No. 2107006.

(27) Qu, X.; Niu, W.; Wang, R.; Li, Z.; Guo, Y.; Liu, X.; Sun, J. Solid-State and Liquid-Free Elastomeric Ionic Conductors with Autonomous Self-Healing Ability. *Mater. Horiz.* **2020**, *7*, 2994−3004.

(28) Li, L.; Zhang, Y.; Lu, H.; Wang, Y.; Xu, J.; Zhu, J.; Zhang, C.; Liu, T. Cryopolymerization Enables Anisotropic Polyaniline Hybrid Hydrogels with Superelasticity and Highly Deformation-Tolerant Electrochemical Energy Storage. *Nat. Commun.* **2020**, *11*, No. 62.

(29) Kang, J.; Tok, J. B. H.; Bao, Z. Self-Healing Soft Electronics. *Nat. Electron.* **2019**, *2*, 144−150.

(30) Wang, Y.; Liu, Y.; Plamthottam, R.; Tebyetekerwa, M.; Xu, J.; Zhu, J.; Zhang, C.; Liu, T. Highly Stretchable and Reconfigurable Ionogels with Unprecedented Thermoplasticity and Ultrafast Self-Healability Enabled by Gradient-Responsive Networks. *Macromolecules* **2021**, *54*, 3832−3844.

(31) Parida, K.; Thangavel, G.; Cai, G.; Zhou, X.; Park, S.; Xiong, J.; Lee, P. S. Extremely Stretchable and Self-Healing Conductor Based on Thermoplastic Elastomer for All-Three-Dimensional Printed Triboelectric Nanogenerator. *Nat. Commun.* **2019**, *10*, No. 2158.

(32) Yin, X.-Y.; Zhang, Y.; Cai, X.; Guo, Q.; Yang, J.; Wang, Z. L. 3D Printing of Ionic Conductors for High-Sensitivity Wearable Sensors. *Mater. Horiz.* **2019**, *6*, 767−780.

(33) Zhang, Y.; Li, M.; Qin, B.; Chen, L.; Liu, Y.; Zhang, X.; Wang, C. Highly Transparent, Underwater Self-Healing, and Ionic Conductive Elastomer Based on Multivalent Ion−Dipole Interactions. *Chem. Mater.* **2020**, *32*, 6310−6317.

(34) He, Y.; Yu, R.; Li, X.; Zhang, M.; Zhang, Y.; Yang, X.; Zhao, X.; Huang, W. Digital Light Processing 4D Printing of Transparent, Strong, Highly Conductive Hydrogels. *ACS Appl. Mater. Interfaces* **2021**, *13*, 36286−36294.

(35) Zhang, B.; Zhang, X.; Wan, K.; Zhu, J.; Xu, J.; Zhang, C.; Liu, T. Dense Hydrogen-Bonding Network Boosts Ionic Conductive Hydrogels with Extremely High Toughness, Rapid Self-Recovery, and Autonomous Adhesion for Human-Motion Detection. *Research* **2021**, *2021*, No. 9761625.

(36) Hou, W.; Luan, Z.; Xie, D.; Zhang, X.; Yu, T.; Sui, K. High Performance Dual Strain-Temperature Sensor Based on Alginate Nanofibril/Graphene Oxide/Polyacrylamide Nanocomposite Hydrogel. *Compos. Commun.* **2021**, *27*, No. 100837.

(37) Shi, L.; Jia, K.; Gao, Y.; Yang, H.; Ma, Y.; Lu, S.; Gao, G.; Bu, H.; Lu, T.; Ding, S. Highly Stretchable and Transparent Ionic Conductor with Novel Hydrophobicity and Extreme-Temperature Tolerance. *Research* **2020**, *2020*, No. 2505619.

(38) Liao, H.; Guo, X. L.; Wan, P. B.; Yu, G. H. Conductive Mxene Nanocomposite Organohydrogel for Flexible, Healable, Low-Temperature Tolerant Strain Sensors. *Adv. Funct. Mater.* **2019**, *29*, No. 1904507.

(39) Wang, J.; Mubarak, S.; Dhamodharan, D.; Divakaran, N.; Wu, L.; Zhang, X. Fabrication of Thermoplastic Functionally Gradient Composite Parts with Anisotropic Thermal Conductive Properties Based on Multicomponent Fused Deposition Modeling 3D Printing. *Compos. Commun.* **2020**, *19*, 142−146.

(40) He, X.; Shi, J.; Hao, Y.; Wang, L.; Qin, X.; Yu, J. PEDOT:PSS/CNT Composites Based Ultra-Stretchable Thermoelectrics and Their Application as Strain Sensors. *Compos. Commun.* **2021**, *27*, No. 100822.

(41) Di, X.; Li, J.; Yang, M. M.; Zhao, Q.; Wu, G. L.; Sun, P. C. Bioinspired, Nucleobase-Driven, Highly Resilient, and Fast-Responsive Antifreeze Ionic Conductive Hydrogels for Durable Pressure and Strain Sensors. *J. Mater. Chem. A* **2021**, *9*, 20703−20713.

(42) Qu, X.; Wang, S.; Zhao, Y.; Huang, H.; Wang, Q.; Shao, J.; Wang, W.; Dong, X. Skin-Inspired Highly Stretchable, Tough and

Adhesive Hydrogels for Tissue-Attached Sensor. *Chem. Eng. J.* **2021**, *425*, No. 131523.

(43) Wang, Z.; Chen, L.; Chen, Y.; Liu, P.; Duan, H.; Cheng, P. 3D Printed Ultrastretchable, Hyper-Antifreezing Conductive Hydrogel for Sensitive Motion and Electrophysiological Signal Monitoring. *Research* **2020**, *2020*, No. 1426078.

(44) Ma, M.; Shang, Y.; Shen, H.; Li, W.; Wang, Q. Highly Transparent Conductive Ionohydrogel for All-Climate Wireless Human-Motion Sensor. *Chem. Eng. J.* **2021**, *420*, No. 129865.

(45) Lu, Y.; Qu, X.; Zhao, W.; Ren, Y.; Si, W.; Wang, W.; Wang, Q.; Huang, W.; Dong, X. Highly Stretchable, Elastic, and Sensitive Mxene-Based Hydrogel for Flexible Strain and Pressure Sensors. *Research* **2020**, *2020*, No. 2038560.

(46) Li, Z.; Zhu, Y. L.; Niu, W.; Yang, X.; Jiang, Z.; Lu, Z. Y.; Liu, X.; Sun, J. Healable and Recyclable Elastomers with Record-High Mechanical Robustness, Unprecedented Crack Tolerance, and Superhigh Elastic Restorability. *Adv. Mater.* **2021**, *33*, No. 2101498.

(47) Xu, L.; Huang, Z.; Deng, Z.; Du, Z.; Sun, T. L.; Guo, Z. H.; Yue, K. A Transparent, Highly Stretchable, Solvent-Resistant, Recyclable Multifunctional Ionogel with Underwater Self-Healing and Adhesion for Reliable Strain Sensors. *Adv. Mater.* **2021**, *33*, No. 2105306.
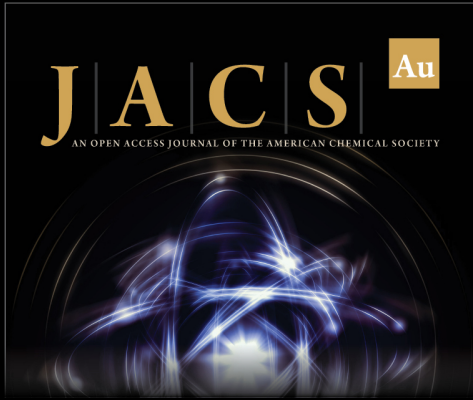
(48) Gao, G.; Yang, F.; Zhou, F.; He, J.; Lu, W.; Xiao, P.; Yan, H.; Pan, C.; Chen, T.; Wang, Z. L. Bioinspired Self-Healing Human-Machine Interactive Touch Pad with Pressure-Sensitive Adhesiveness on Targeted Substrates. *Adv. Mater.* **2020**, *32*, No. 2004290.

(49) Shi, P.; Wang, Y.; Tjiu, W. W.; Zhang, C.; Liu, T. Highly Stretchable, Fast Self-Healing, and Waterproof Fluorinated Copolymer Ionogels with Selectively Enriched Ionic Liquids for Human-Motion Detection. *ACS Appl. Mater. Interfaces* **2021**, *13*, 49358−49368.

(50) Dong, X.; Wu, Z.; Wang, Y.; Li, T.; Yuan, H.; Zhang, X.; Ma, P.; Chen, M.; Dong, W. Design of Degradable Core-Shell Starch Nanoparticles by Radical Ring-Opening Polymerization of 2-Methylene-1,3-Dioxepane and Their Toughening of Poly (Lactic Acid). *Compos. Commun.* **2021**, *27*, No. 100808.

(51) Scheiger, J. M.; Li, S.; Brehm, M.; Bartschat, A.; Theato, P.; Levkin, P. A. Inherently UV Photodegradable Poly(Methacrylate) Gels. *Adv. Funct. Mater.* **2021**, *31*, No. 2105681.

(52) Li, Y.; Li, S.; Sun, J. Degradable Poly(Vinyl Alcohol)-Based Supramolecular Plastics with High Mechanical Strength in a Watery Environment. *Adv. Mater.* **2021**, *33*, No. 2007371.